CHAPTER IV
RESULTS AND DISCUSSION

Physical properties of sol-gel aluminas prepared were determined through BET surface area measurement, thermalgravimetric analysis (TGA), and X-ray diffraction technique. Moreover, adsorption behaviors of these adsorbents on the dynamic water and hydrocarbons adsorption were also studied. Details and discussion over these practical results together with informative figures will be presented in this section.

4.1 Adsorbent Characterization

The synthesis of sol-gel aluminas used in this work was done by the hydrolysis of aluminum alkoxide at 85°C. Fresh adsorbents were immediately tested for their physical properties. For the adsorbent characterization, the effects of calcination temperature and time on the adsorbent properties were studied. Aluminas were prepared and calcined at 400, 500, 600, and 700°C for 5, 6, and 6.5 hours. The aluminas prepared in the range of the calcination temperature and time are in the gamma form (γ-Al_2O_3), which possesses high surface area (Perason and Grant, 1992).

Calcination is a further heat-treatment step, beyond drying, during the adsorbent preparation process. Normally, calcination is referred to the calcination in contact with air, typically at temperature higher than those used in the adsorbent pretreatment and regeneration. Several processes occur during calcination. They include loss of chemically bonded water and some gases like CO_2, modification of the texture through sintering, modification of adsorbent structure, active phase generation, and stabilization of mechanical properties (Perego and Villa, 1997).

4.1.1 Effects of Calcination Temperature on the Adsorbent Properties

BET Surface Area and Pore Size Distribution

Summarized data of the BET surface area, total pore volume, and average pore size of the prepared sol-gel aluminas are shown in Table 4.1. In this study, the calcination temperature was varied from 400 to 700°C. At the same calcination time, the BET surface areas of these aluminas decrease with increasing the calcination temperature. As shown in Table 4.1, the surface area of the sol-gel alumina calcined at 400°C is twice as much as that calcined at 700°C. Over the range of the calcination temperature and time studied, the sol-gel alumina calcined at 400°C for 5 hours had the highest BET surface area of 573 m^2/g.

The pore volume and pore size of these sol-gel aluminas were also investigated. According to Table 4.1, the maximum pore volume of 0.19 cm^3/g is obtained for the sol-gel alumina calcined at 400°C for 5 hours. Like the BET surface area, the overall pore volume reduced with increasing calcination temperature. For the pore size, all prepared sol-gel aluminas had very small pore radius between 6.7 to 7.4 angstroms. The values of the pore radius indicate that these sol-gel aluminas were microporous materials.

The reduction of BET surface area and the decrease in the total pore volume of the prepared sol-gel aluminas, it implies that both phenomena are resulted from the sintering effect of the alumina structure during the calcination process at high temperature (Perego and Villa, 1997). In case of alumina, upon the calcination of bohemite above 300°C, a series of phase changes occur, simultaneously, with the loss of hydroxyl groups and hence of water. These result in the formation of a series of oxides ($\eta-$, $\gamma-$, and $\delta-$ phase), known as pseudo $\gamma-$alumina (Perego and Villa, 1997), which is good for binder, catalyst support, and even adsorbent. Further increasing calcination temperature will enhance the sintering process and result in a sharp

Table 4.1 Effects of calcination temperature and calcination time on BET surface area and pore size distribution of the sol-gel alumina.

Calcination Temperature (°C)	Calcination Time (hr)	BET Surface Area* (m^2/g)	Pore Volume‡ (cm^3/g)	Pore Radius§ (°A)
400	5.0	573	0.19	5.9
400	6.0	552	0.18	6.7
400	6.5	509	0.17	6.7
500	5.0	517	0.18	6.6
500	6.0	458	0.17	6.8
500	6.5	435	0.16	6.8
600	5.0	362	0.13	7.1
600	6.0	358	0.12	7.2
600	6.5	332	0.12	7.3
700	5.0	303	0.11	7.3
700	6.0	275	0.10	7.4
700	6.5	284	0.10	7.6

* : From 5 point BET

‡ : Total pore volume for pores with radius less than 8 °A at $P/P_o = 0.1064$

§ : Average pore radius

drop of the total surface area of alumina. If the calcination temperature increased to above 900°C, the monoclinic $\theta-Al_2O_3$ will form and it will transform into the hexagonal $\alpha-Al_2O_3$ if the calcination temperature reaches 1,200°C. These materials are anhydrous, low surface area oxides and are not suitable for adsorbent purposes. They are used in applications where the mechanical strength is required (Perego and Villa, 1997).

Changing the calcination temperature, even when the phase transitions are avoided, can affect the material pore size. For gamma alumina, increasing the calcination temperature results in a collapse of micropores, and this increases the mean pore size (Richardson, 1989).

Water Adsorption Capacity

Determination of total water adsorption capacity was done through the use of thermalgravimetric analyzer (TGA). The net water adsorbed of each sol-gel alumina is shown in Table 4.2. The total water adsorption capacity was examined based on the alumina's dry weight compared to the net weight gained during its isothermal adsorption. As seen in Table 4.2, an obvious drop in the amount of water adsorbed occurs as the calcination temperature increases. This effect results from the reduction of the total pore volume of the sol-gel alumina as the calcination temperature increases. Again, the sol-gel alumina, which was calcined at 400°C for 5 hours, gave the highest water adsorption capacity (0.19 g/g of alumina).

Comparison of the pore volume and pore radius data in Table 4.1 and the water adsorption capacity in Table 4.2 shows that, at the low calcination temperature, where the sol-gel aluminas have very small pore radius, the water adsorption capacity is close to the total pore volume. When the calcination temperature increases, which, in turn, increases the pore size. There is a gradually increase in the difference between the pore volume and the water adsorption capacity. From this observation, it can be postulated that the capillary effect plays an important role in the water adsorption mechanism

Table 4.2 Water adsorption capacity of the sol-gel alumina prepared at various calcination temperatures and calcination times.

Calcination Temperature (°C)	Calcination Time (hr)	Water Adsorption Capacity (g/g of alumina)
400	5.0	0.199
400	6.0	0.165
400	6.5	0.150
500	5.0	0.152
500	6.0	0.143
500	6.5	0.139
600	5.0	0.085
600	6.0	0.076
600	6.5	0.064
700	5.0	0.085
700	6.0	0.068
700	6.5	0.064

of these sol-gel aluminas. The capillary effect is the condensation of vapor to liquid in specific small cylinders or pores. The condensed liquid occupies almost all pore volume of the porous material. This mechanism results in high water adsorption capacity.

XRD Analysis

Figure 4.1 shows the comparison of the X-ray diffraction patterns of the sol-gel aluminas prepared with different calcination temperatures together with the uncalcined alumina. The X-ray diffraction pattern of an commercial gamma alumina sample obtained from the Alfa Chemical Co., Ltd. was also compared in this figure. The pattern of the uncalcined material exhibits the absolutely amorphous solid structure. After calcination at high temperature, the modification of the solid took place. This can be evidently shown by the difference of the XRD patterns of aluminas before and after the calcination. For all these sol-gel aluminas, their XRD patterns correspond to the gamma alumina of amorphous structure. Peaks of these patterns at 2θ value equal to 37.0, 46.2, and 67.1 indicate the gamma form of these sol-gel aluminas.

When the calcaination temperature increases, the shape of the peaks, especially at 2θ value of 46.2, and 67.1, is significantly sharper. Normally, the smoothness and sharpness of the X-ray diffraction patterns indicate the crystallinity of the solid. For alumina, as the calcination temperature increase, the structure of alumina is modified to be more crystalline solid. If the calcination temperature increases to about 900°C, the structure of alumina is totally changed to monoclinic θ–Al_2O_3 form and transforms into hexagonal α–Al_2O_3 if the calcination temperature reaches 1,200°C (Richardson, 1989).

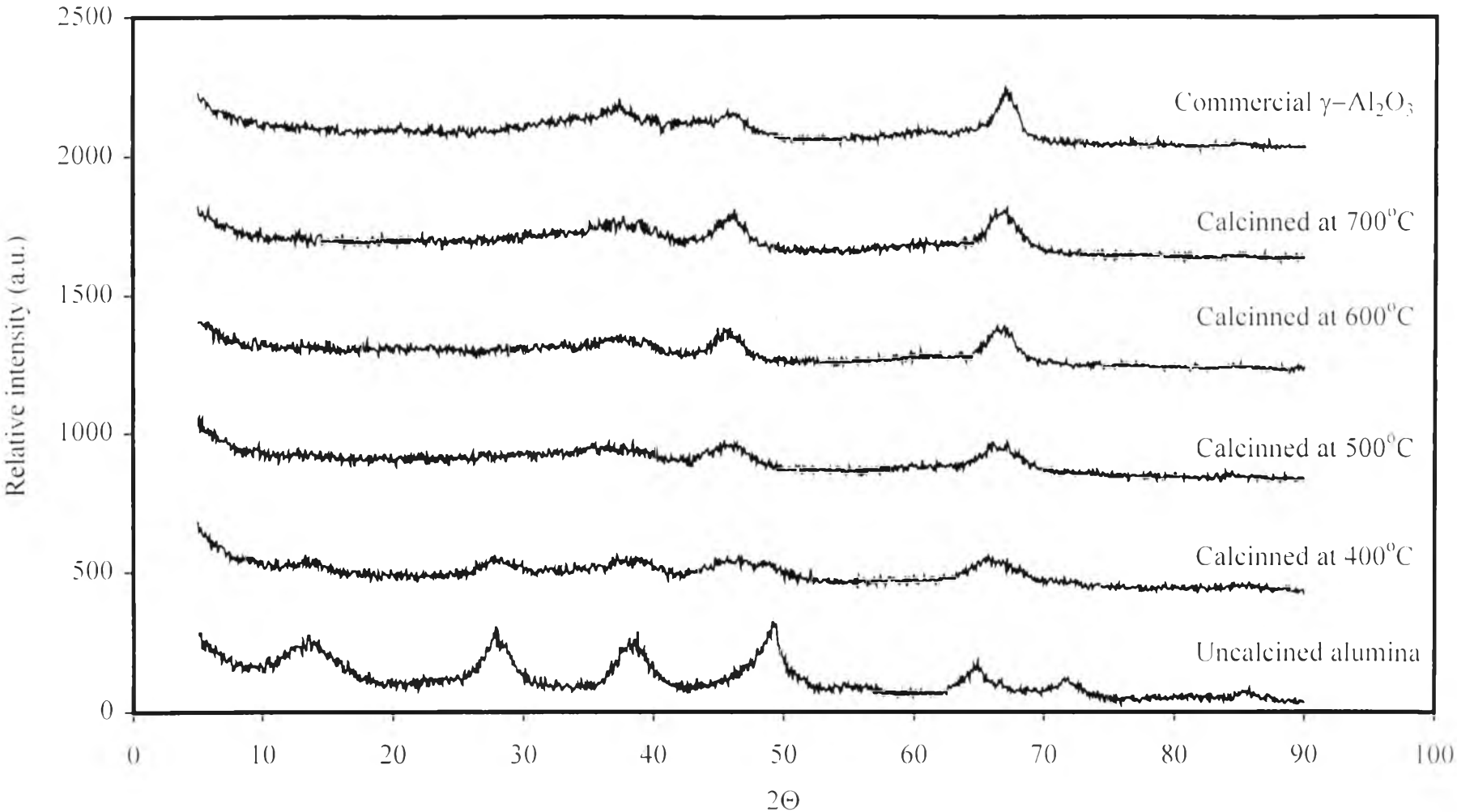

Figure 4.1 XRD patterns of the sol-gel alumina calcined at for 5 hours at various calcination temperatures.

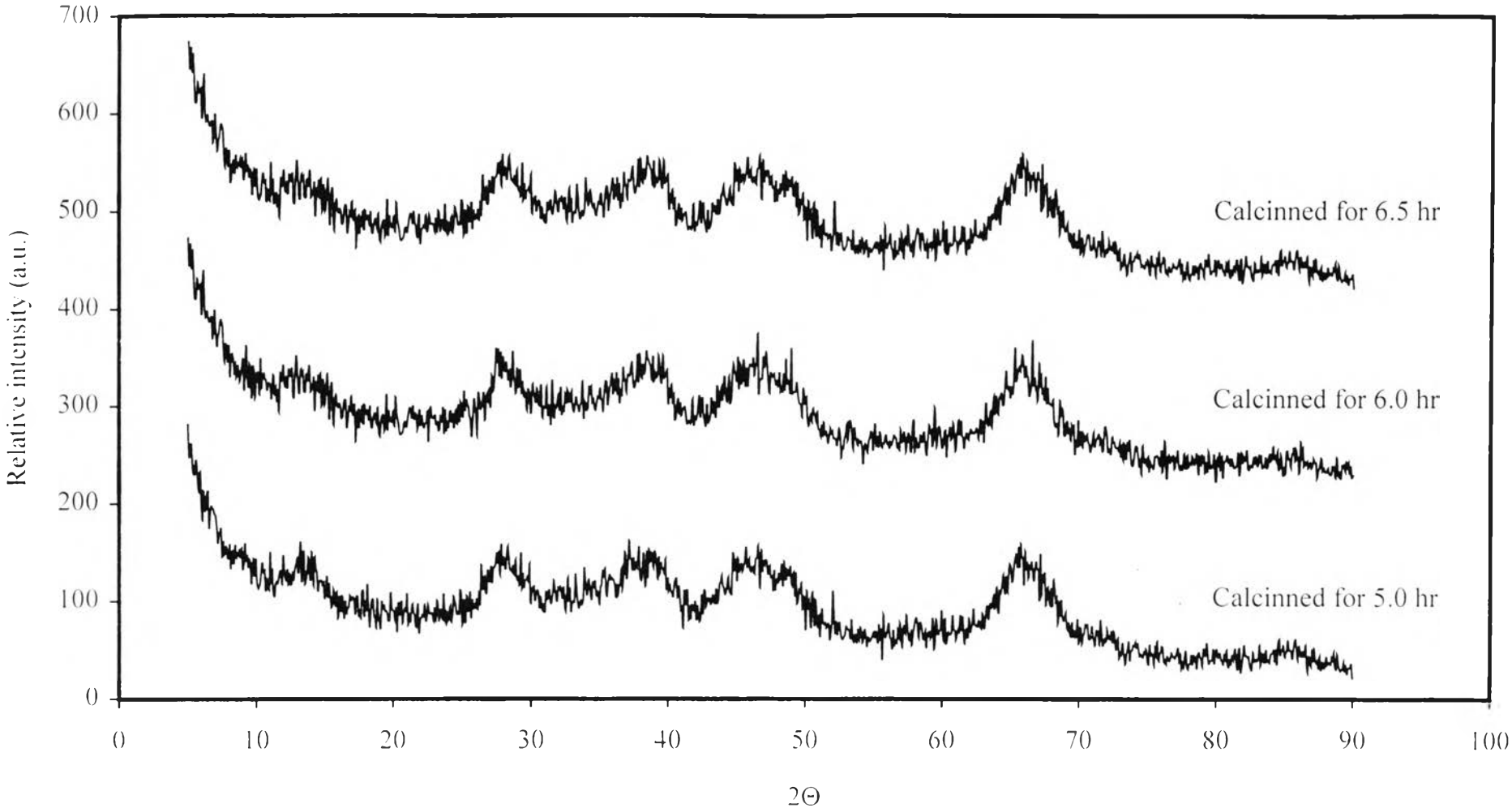

Figure 4.2 XRD patterns of the sol-gel alumina calcined at 400°C with different calcination time.

4.1.2 Effects of Calcination Time on the Adsorbent Properties

BET Surface Area and Pore Size Distribution

Table 4.1 shows that, with the same calcination temperature, different calcination times result in different physical properties of the sol-gel alumina. When the calcination time increased, a remarkable drop in the BET surface area was observed. The pore volume also follows the same trend as that of the surface area. When the calcination time increased, the total pore volume decreased, but the average pore radius increased. It can be concluded that all these changes correspond to the general sintering effect during the heat treatment of the sol-gel alumina structure. The long period of time during the calcination enhances the change of the adsorbent texture.

Water Adsorption Capacity

As mentioned before, the total pore volume of these sol-gel aluminas decreased and the pore size increased with increasing the calcination time. These affect the water adsorption capacity of water. As seen in Table 4.2, when the calcination time increases, the adsorption capacity drops, dramatically. Since the capillary effect was found to be an important mechanism in the water adsorption of this sol-gel alumina, an increase in pore size will inhibit these phenomena, and this results in a significant decrease in the water adsorption capacity.

XRD Analysis

The XRD-patterns of the sol-gel alumina calcined at 400°C with different calcination time are shown in Figure 4.2. From this figure, no significant difference between each XRD pattern could be observed. This may be because the range of the calcination times studied in this experiment hardly affect the alumina crystalline structure. Normally, when the calcination time increases, it will enhance the modification of adsorbent morphology. This will result in a lower BET surface area, reduction of total pore volume and pore size of alumina.

4.2 Competitive Adsorption of Water and Hydrocarbons in the Simulated Natural Gas System

In this part, the focus shifts to the adsorption mechanism of gases, both water and hydrocarbons, in the simulated natural gas system. The multicomponent adsorption experiments were carried out only with the highest surface area alumina (calcined at 400°C for 5 hr). The natural gas used in this study consisted of several hydrocarbon compounds including, methane (CH_4), ethane (C_2H_6), propane (C_3H_8), iso- and n-butane (C_4H_{10}). All the hydrocarbons in the natural gas stream represented light hydrocarbons. The representation of a heavy hydrocarbon used here was pentane.

Figure 4.3 shows the breakthrough curves of water and hydrocarbons in this adsorption system. Normally, a breakthrough curve shows the relation between the ratio of concentration of an interested component at anytime (C_t) to that of the component in the feed (C_i) and the adsorption time. From Figure 4.3, for water, the term C_t/C_i gradually increases and reaches the value of one and remains constant, but for all hydrocarbons C_t/C_i can go beyond one, the Roll-Up effect. More details of this phenomenon have been described by Ruthven (1984).

The Roll-Up phenomenon occurs via the replacement of low molecular weight molecules by higher molecular weight molecules or the replacement of low affinity molecules by molecules with higher affinity. To prove this mechanism, first, an experiment was done by the adsorption of the hydrocarbons only, without the presence of water. Until the alumina bed was saturated with the hydrocarbons, which could be observed that the inlet and outlet hydrocarbon compositions is equal. Then the adsorbent bed was purged with pure nitrogen gas for a while to remove the residue hydrocarbons left. Next, the humidified nitrogen gas was introduced to the column to start the water adsorption. With this technique, if the proposed hypothesis is correct,

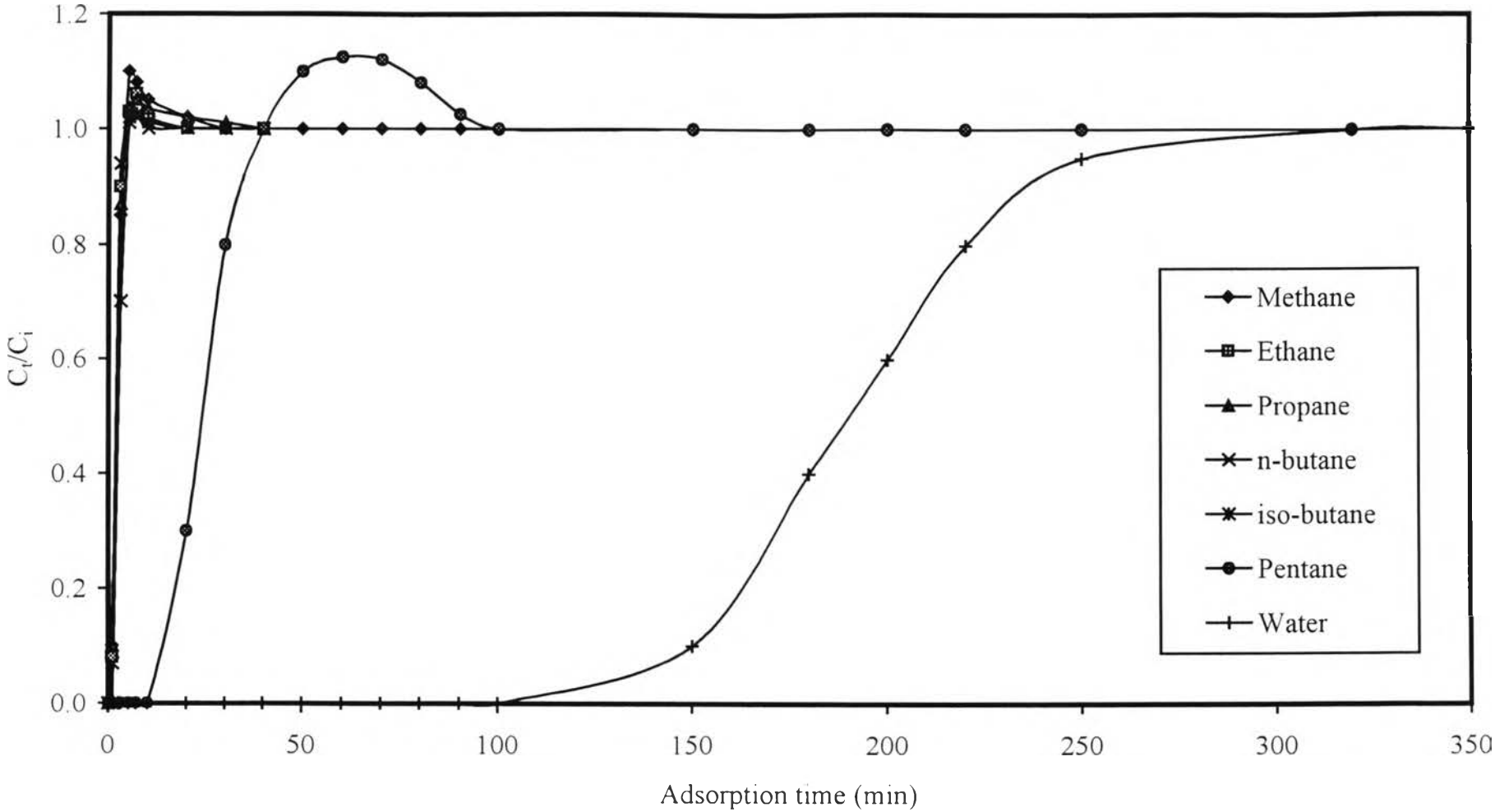

Figure 4.3 Breakthrough curves of water and hydrocarbons adsorbed on the sol-gel alumina at 30°C.

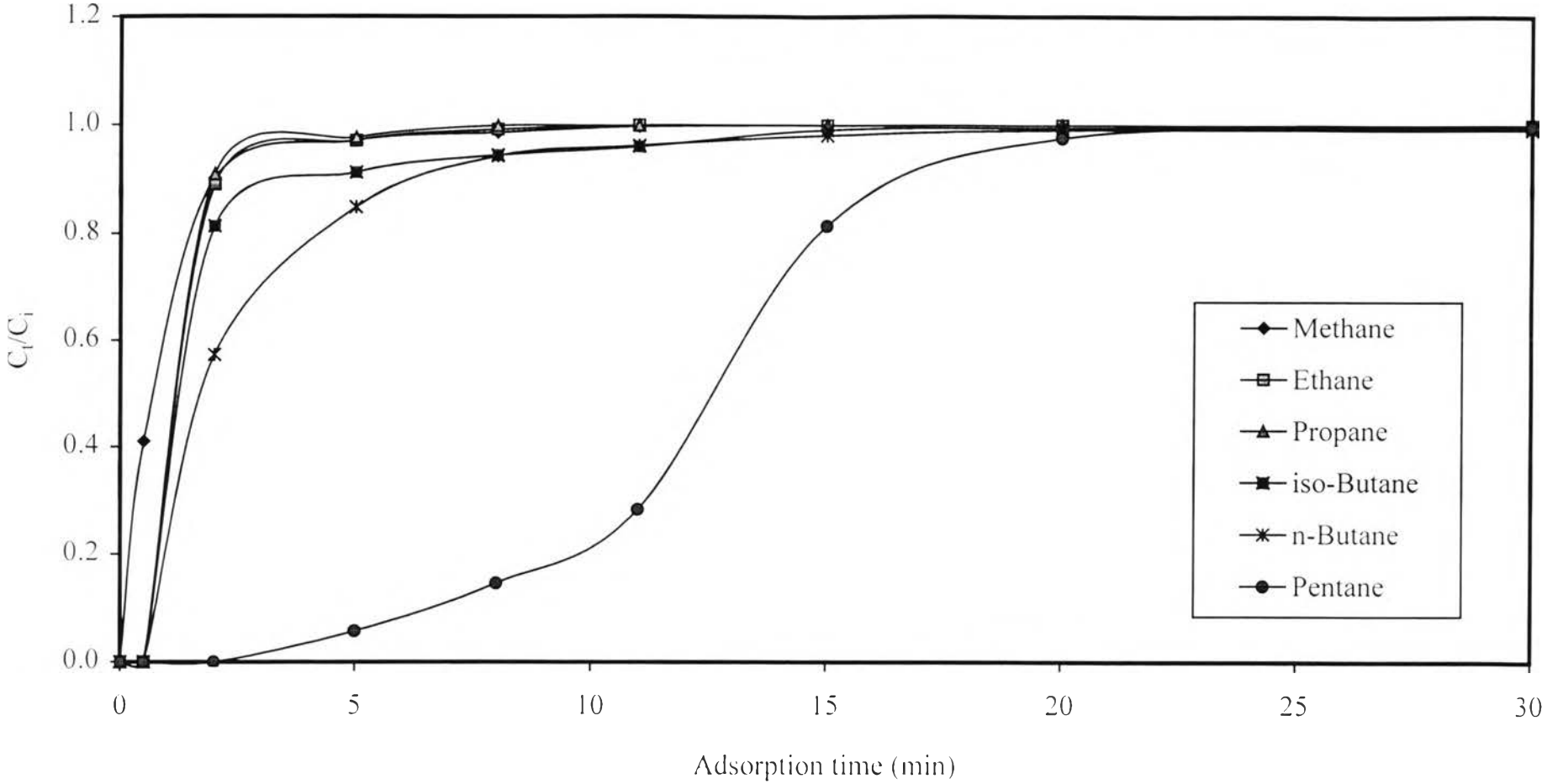

Figure 4.4 Breakthrough curves of hydrocarbons adsorbed on the sol-gel alumina at 30°C without water.

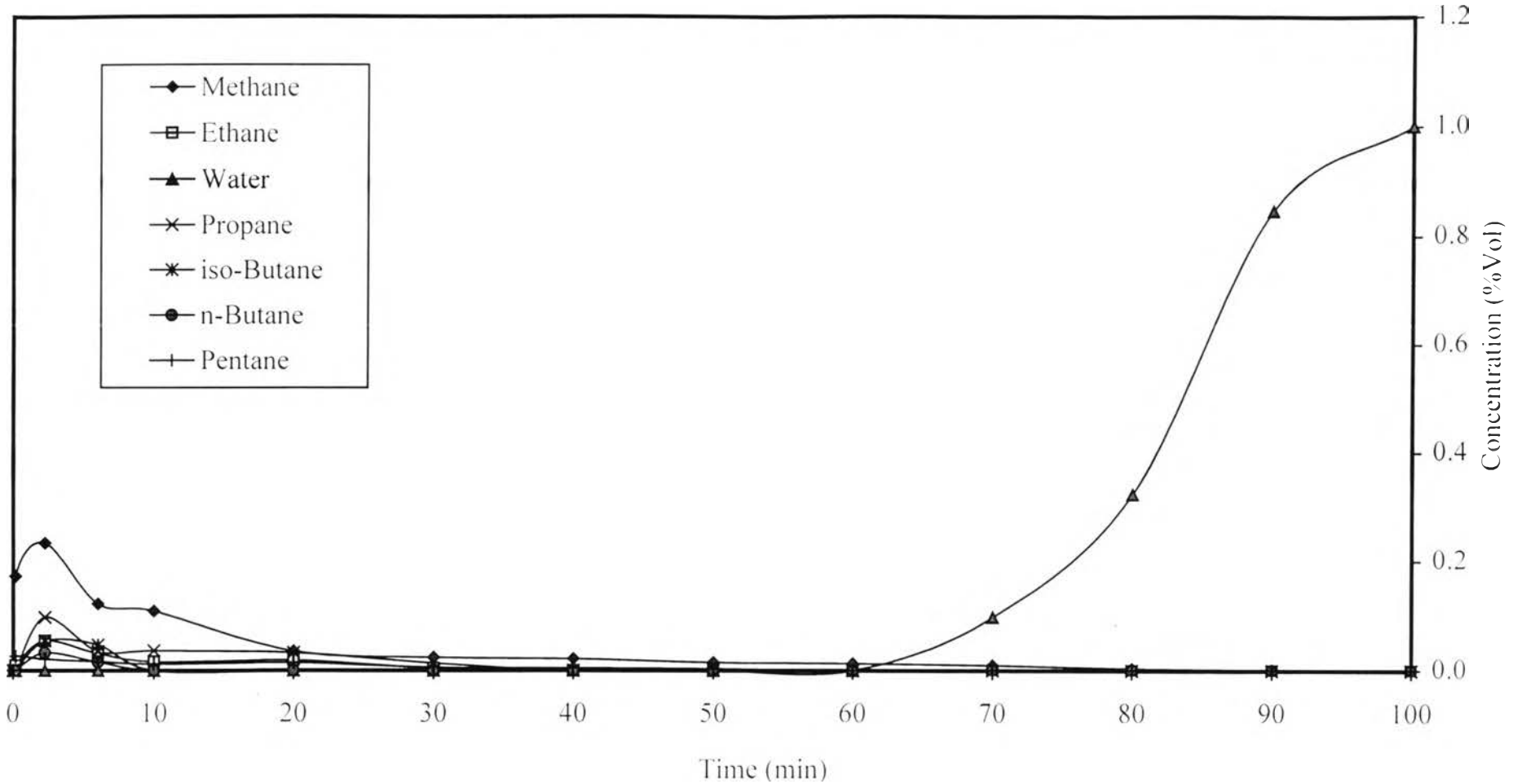

Figure 4.5 Concentration of the outlet gas in the water replacement test.

once the adsorption of water begin, hydrocarbon should be detected at the outlet of the adsorption column.

Figure 4.4 demonstrates the breakthrough curve of all hydrocarbons during the first step of this experiment. At this step, no water appeared in the gas stream. All breakthrough curves gradually increased and reached the value of one. The plots exhibit different than in the case we have water in the gas stream as seen in Figure 4.3. No roll up effect can be observed. This phenomenon proves that, there is no replacement between the hydrocarbons itself along the adsorption on the sol-gel alumina surface.

Figure 4.5 shows the concentrations of the components came out from the adsorption column immediately after the humidified nitrogen flow was introduced into column. The figure shows that a certain amount of hydrocarbon can be detected at the very beginning. Methane has the highest concentration since it is the major component in the natural gas used. The data obtained from this figure can explain that, at the very beginning of the adsorption process, hydrocarbon molecules are adsorbed onto the alumina surface, but dramatically desorped out later because of the replacement of water molecules, which possess higher affinity than the hydrocarbons. The hydrocarbon molecules are finally desorbed into the gas stream and came out of the adsorbent bed. This effect resulted in increasing the hydrocarbon concentration in the outlet stream, which was even higher than the inlet concentration.

4.2.1 Adsorption Behaviors of Hydrocarbons

Figure 4.6 shows the adsorption isotherms of methane, ethane, propane, iso-butane, n-butane, and pentane on the sol-gel alumina obtained from the adsorption of the simulated natural gas system. The sol-gel alumina used in this experiment was calcined at 400°C for 5 hours and has the highest BET surface area, total pore volume, and water desorption capacity. From

Figure 4.6, it can be said that as the molecular weight of the adsorbate increases, the relative amount adsorbed also increases. There are several reasons for this behavior.

Table 4.3 shows the amounts of each gas adsorbed on the alumina surface and concentration of each gas in the gas stream used in the adsorption. The data resulted from the adsorption experiment of the constant concentration of natural gas at 5% vol, water vapor at 1%, and pentane at 0.5%. For the same type of adsorbate, the adsorption behavior is determined by the van der Waal interaction between the adsorbate and the surface. An increase in the molecular weight enhances the physisorption capacity. According to Table 4.3, the amount of methane adsorbed to its concentration in the gas phase ratio is 4.267×10^{-3},while that of ethane and propane are 10.098×10^{-3} and 15.593×10^{-3}, respectively. It means that an increase in each -CH_2 group increases the ratio for about 0.005. In case of normal and iso-butane, their ratio are slightly different because of their molecular shape.

The isotherm of pentane in Figure 4.6 is different from the other hydrocarbons. The boiling point of pentane is 36.1°C and the adsorption experiment was done at 30°C. Thus, pentane condensed during the adsorption. This makes the isotherm of pentane behaves differently from the other linear alkanes. To determine the concentration of pentane, at which the condensation starts, the Kelvin's equation can be used.

In a porous adsorbent, there is a continuous progression from multilayer adsorption to capillary condensation, in which the small pores are completely filled with liquid sorbate. This occurs because the saturation vapor pressure in a small pore is reduced by the effect of surface tension. The details calculation of the capillary condensation of pentane is clearly shown in Appendix. The calculation shows that the capillary condensation of pentane on this sol-gel alumina starts at the concentration of pentane in the gas phase equal to 7.9% vol.

Table 4.3 Adsorption capacity of hydrocarbons on the sol-gel alumina surface.

Composition	Amount Adsorbed x 10^{3} (g/g of alumina)	Concentration in the Gas Stream x 10^{2} (% Vol/100)	Ratio of Amount Adsorbed per Concentration in Gas Phase x 10^{3}
Methane	0.145	3.391	4.276
Ethane	0.067	0.664	10.098
Propane	0.092	0.590	15.593
iso-Butane	0.122	0.210	58.095
n-Butane	0.057	0.146	39.125
Pentane	4.100	0.500	820.000

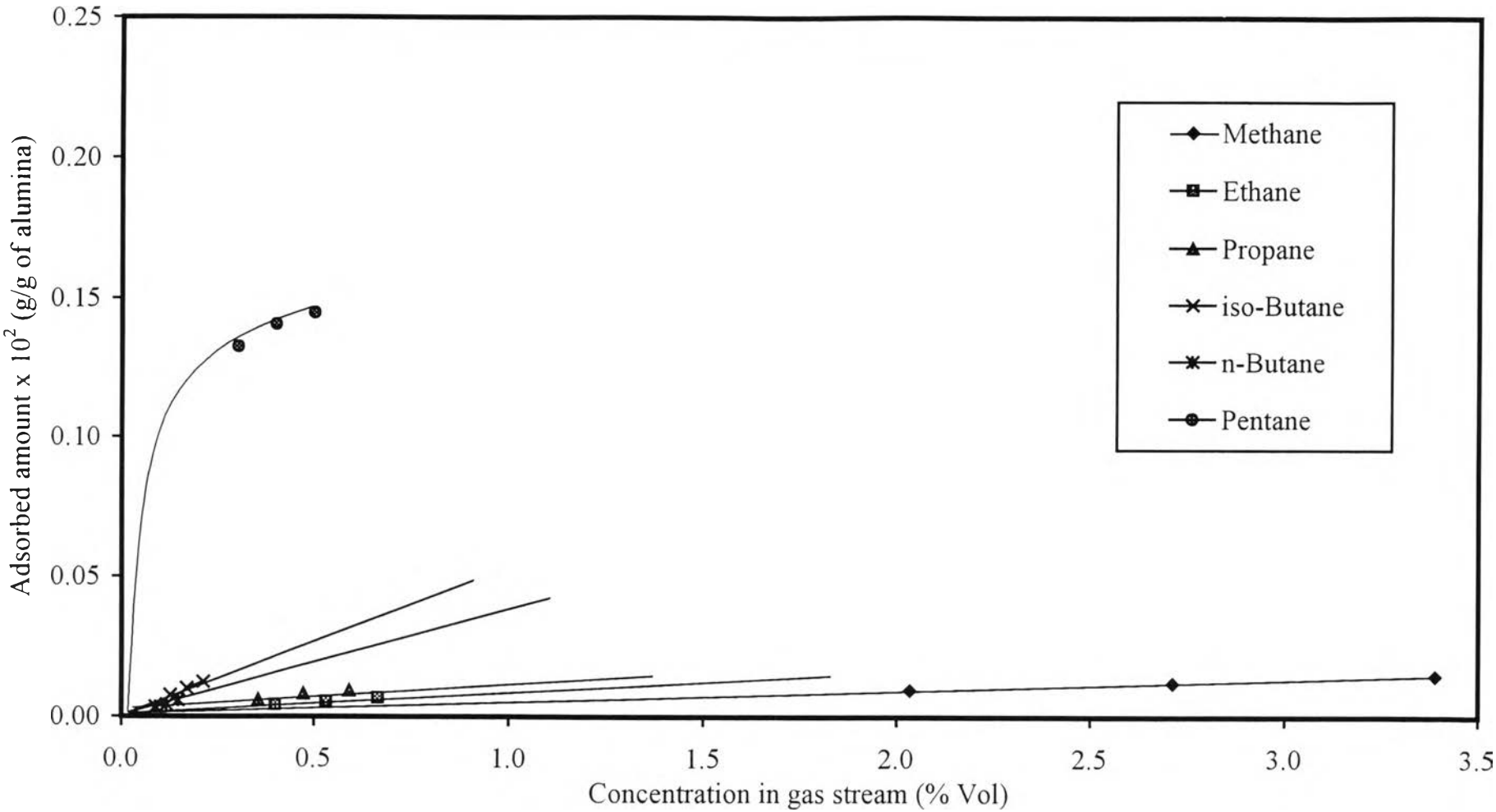

Figure 4.6 Adsorption isotherms of hydrocarbons on the sol-gel alumina at 30°C.

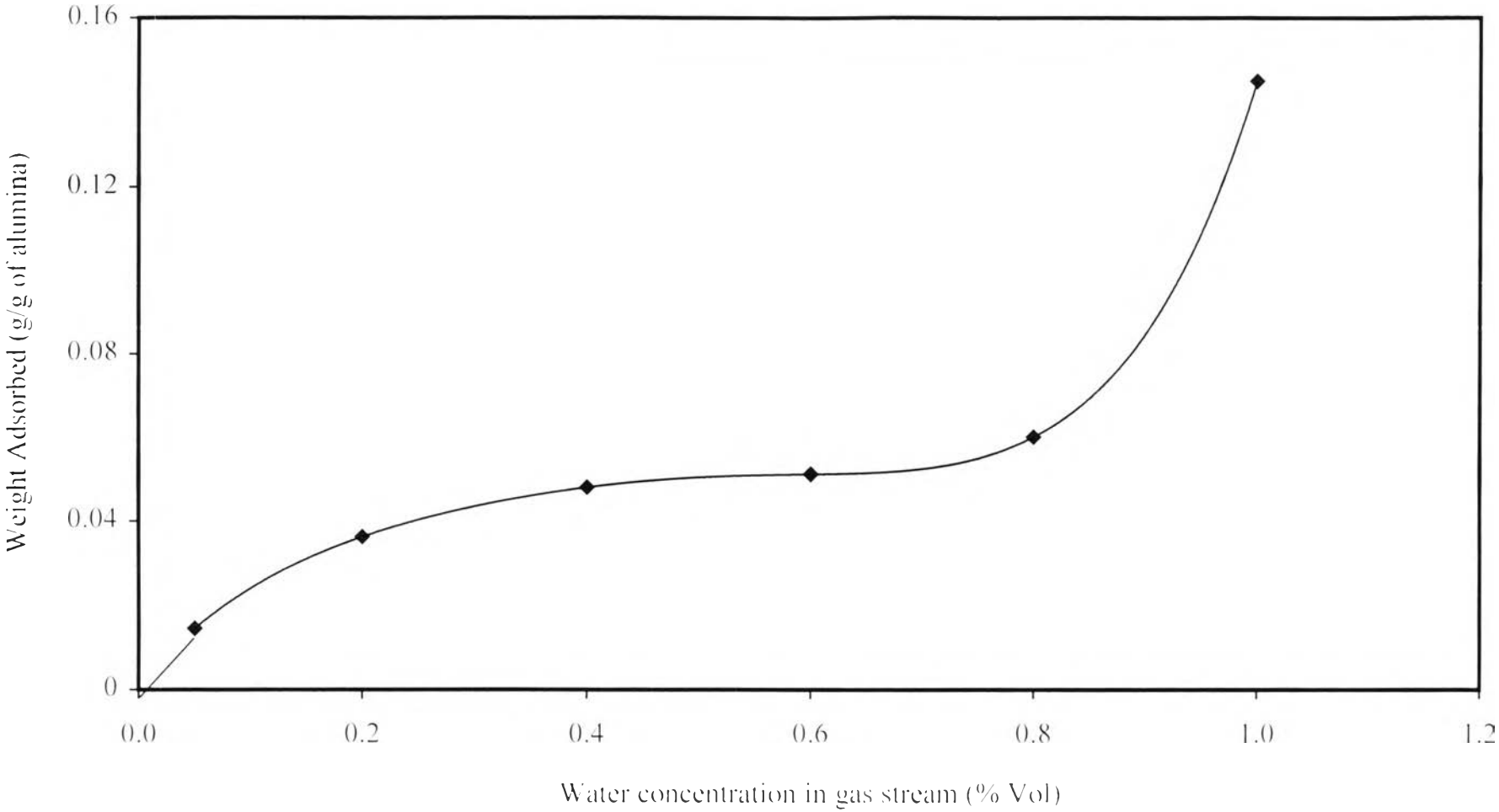

Figure 4.7 Adsorption isotherm of water on the sol-gel alumina at 30°C.

Even pentane was adsorbed with higher amount than the others hydrocarbons, the water replacement effect was also observed. However, the data from the breakthrough plot of pentane during the adsorption process implies that pentane has stronger affinity than the other hydrocarbons because the breakthrough time of pentane is higher than that of the other hydrocarbons.

4.2.2 Adsorption Behaviors of Water

Figure 4.7 shows the dynamic adsorption isotherm of water on the sol-gel alumina calcined at 400°C for 5 hours. The adsorption was done at 30°C, which is the real application temperature using in the gas separation process. The resulted isotherm shows the type II Brunauer isotherm or sometimes called the sigmoid or S-shaped isotherm (Satterfield, 1991). The isotherm indicates that there is a continuous progression of water adsorption from monolayer to multilayer and then to capillary condensation. The increase in the adsorbed capacity at high pressure is due to the capillary condensation in the pores as the adsorbate portion raised (Ruthven, 1984). Details of capillary condensation calculation using the Kelvin's equation are shown in Appendix. From this calculation, it revealed that, for this sol-gel alumina, water vapor starts to condense in the micropores at the concentration of water in the gas phase equal to 0.8% vol.

In this study, at the same condition, the amount of water adsorbed was several times greater than those of hydrocarbons. This substantiates that water molecule has higher affinity compared to hydrocarbons. The dynamic water adsorption is, in fact, involved with several overlap phenomena (Nedez *et al.*, 1996). The clear initial increase in the isotherm corresponds to the chemisorption of water molecules on the alumina surface. This is the monolayer adsorption stage. Then, the formation of growing multilayers of water vapor follows. In the small pore materials, according to the Kelvin's equation, the saturated vapor pressure is lowered,

which eventually transforms water vapor into liquid (Ponee *et al.*, 1974). Therefore, the beginning of capillary condensation coincides with the sharp inflection of the adsorption isotherm as seen in Figure 4.7.

The Al-O bonds are more ionic than the covalent bond so the surface charges vary in intensity. As the water is added to the alumina surface, hydrogen bonding between the adjacent adsorbed water molecules was immediately developed. At the same time, the hydrogen bonds are formed between the adsorbed water molecules and the free water molecules in the gas stream. Although the accurate nature of these hydrogen bonds is not yet well understood, it has been usually treated this phenomena as physisorption (Nedez *et al.*, 1996). This effect is referred to the start of capillary condensation. So, it can be concluded that the water adsorption is the combination of three different effects, first with the generation of monolayer chemisorption, followed by the multilayers of physisorption of water vapor, and completed with the capillary condensation.

4.2.3 Effects of Water Composition on the Overall Adsorption Process

One objective of this study was to determine the effect of water and hydrocarbons concentrations on the adsorption behavior of other species. For this reason, the concentration of each component was varied; 3-5% of natural gas, 0.05-1% for water, and 0.3-0.5% for pentane. In this section, since all hydrocarbons in the natural gas stream exhibit almost the same behavior, methane was used to represent the behavior of all gases in the natural gas stream. Three components; natural gas (methane), heavy hydrocarbon (pentane) and water, were, then, varied in this study.

Figure 4.8 shows the comparison of the breakthrough curves of methane with different water concentrations. When the amount of water increased the breakthrough time of methane reduced. The same holds true for the case of pentane as shown in Figure 4.9. This result also supports that the

the strong affinity of water with alumina surface has a great effect on the replacement of hydrocarbons, which have weak affinity, during the competitive adsorption.

4.2.4 Effects of Hydrocarbons Composition on the Overall Adsorption Process

Figure 4.10 shows the breakthrough curves of water adsorption with various light hydrocarbon concentrations. The plots do not show a significant difference in each curve. The breakthrough time of water at different natural gas concentration is almost the same. The same is also true for the breakthrough plots of pentane as indicated in Figure 4.11. This means the variation of natural gas composition in this range of study (3-5 %) has no effect on the adsorption behaviors of the other species on the sol-gel alumina surface.

The same phenomena are observed here for varying of pentane concentration as shown in Figures 4.12 and 4.13. This indicates that by varying the pentane composition from 0.3 to 0.5% has little effect on the adsorption behavior of water and other hydrocarbons on the sol-gel alumina surface during the adsorption process at 30°C.

4.3 Adsorbent Regeneration

Regeneration of adsorbent is also an important step of the adsorption process. Adsorbent, which requires less energy for regeneration, is the most desirable material. The thermogram obtained during the regeneration of the water-saturated alumina is shown in Figure 4.14. The plot also shows the derivative between total adsorbent weight change and temperature. The great drop of the derivative curve at the position around 100°C indicates that almost all water vapor that adsorbed in this alumina amount is caused by the

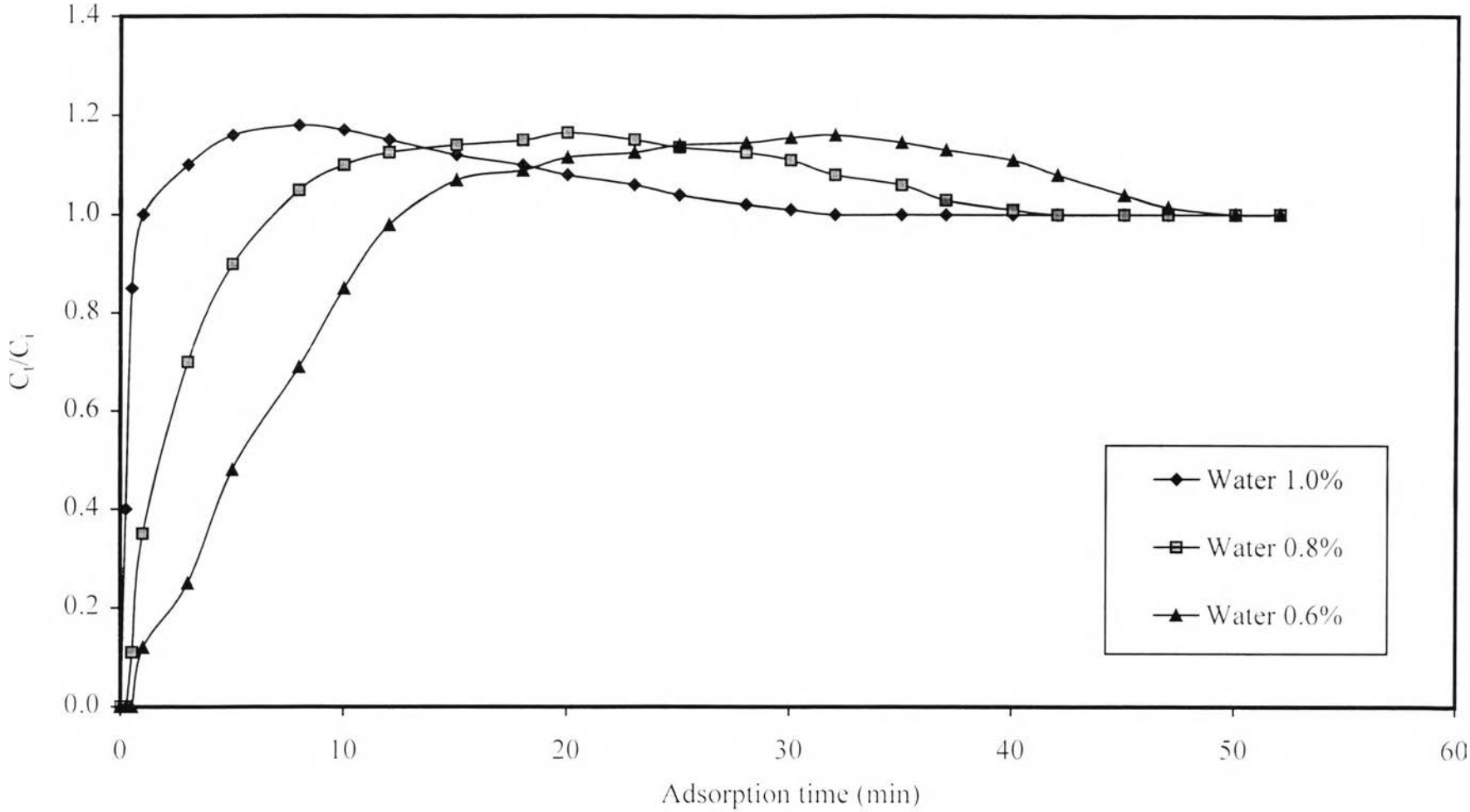

Figure 4.8 Breakthroug curves of methane with different water concentration.

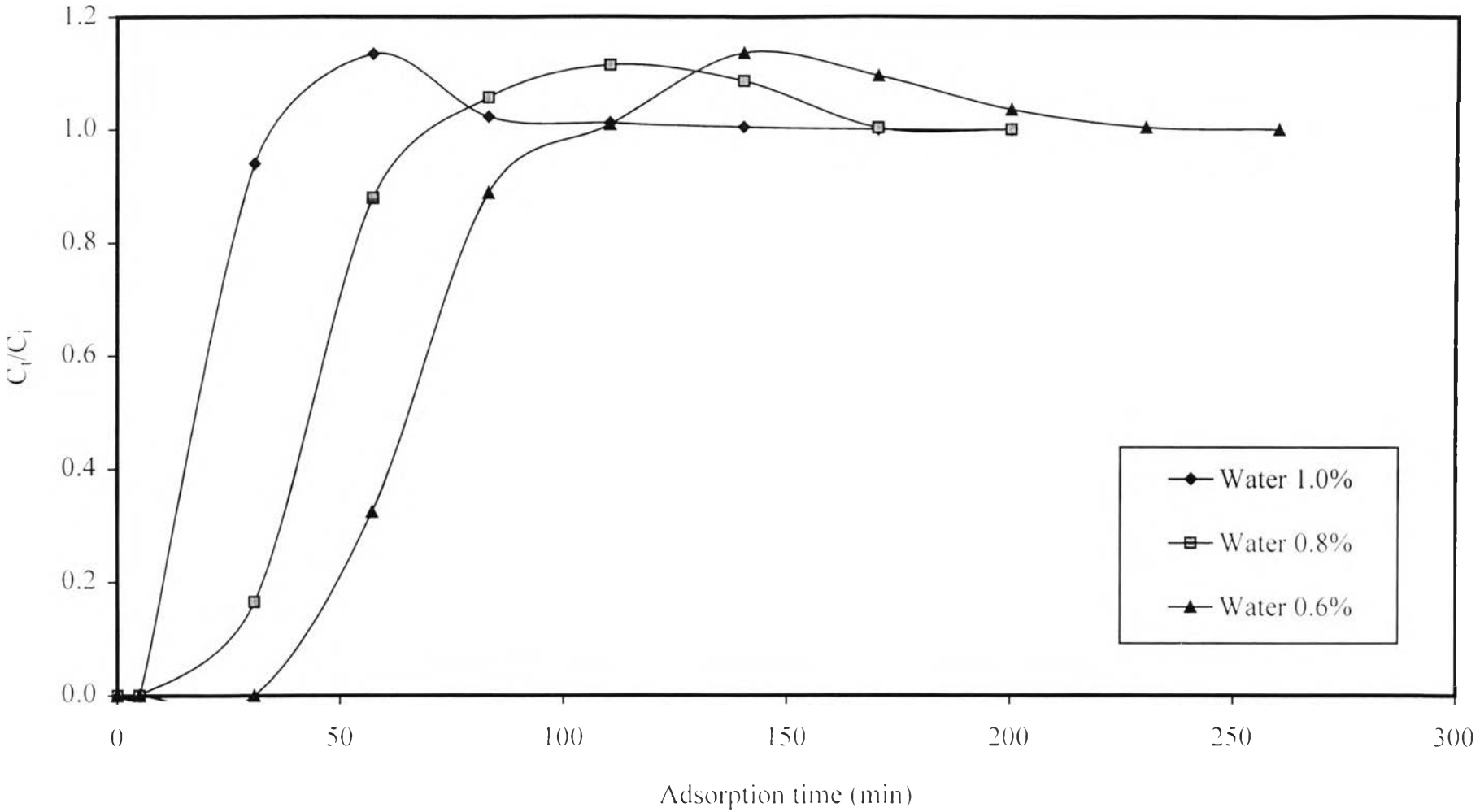

Figure 4.9 Breakthrough curves of pentane with different water concentration.

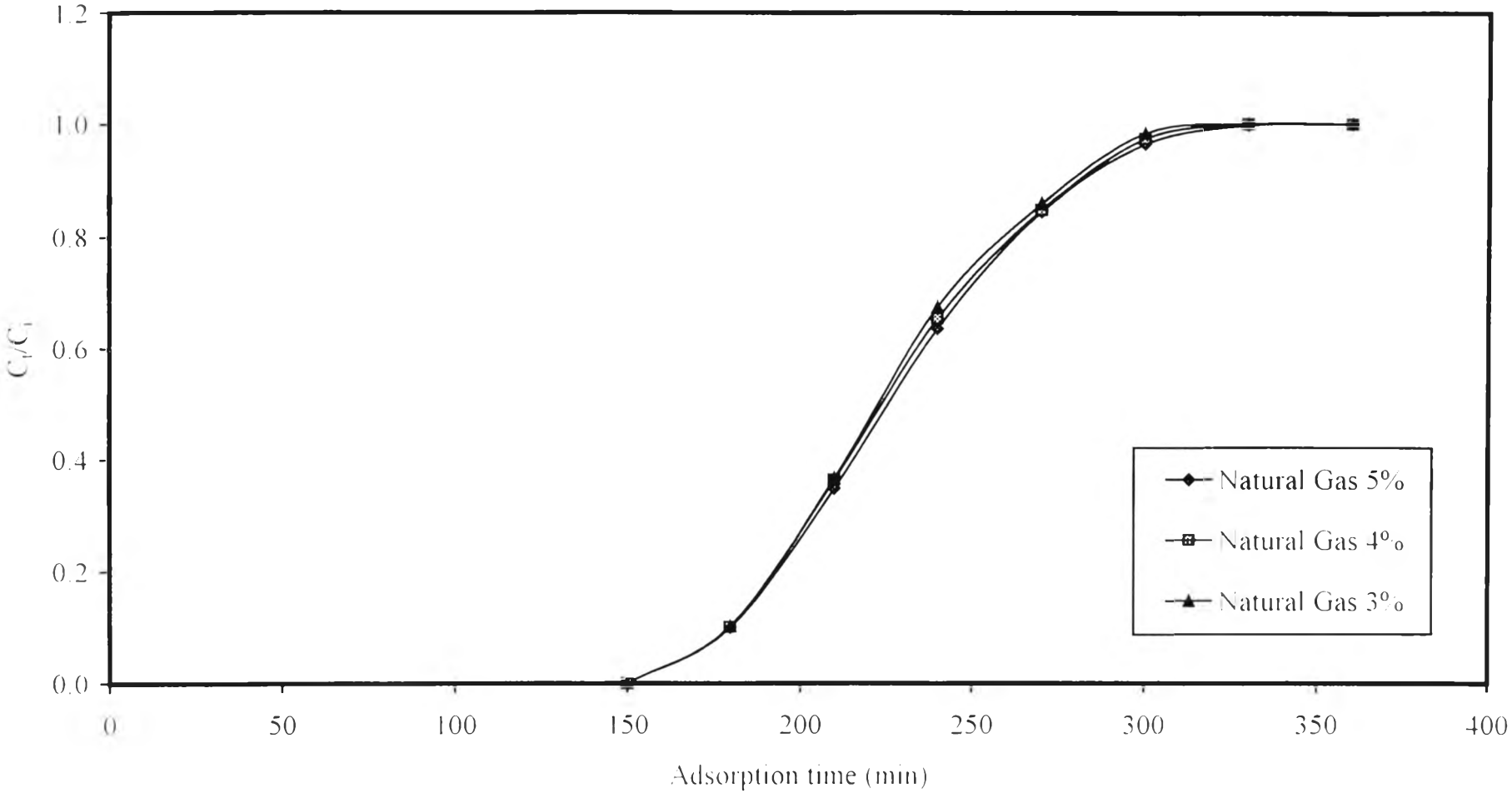

Figure 4.10 Breakthrough curves of water with different natural gas concentration.

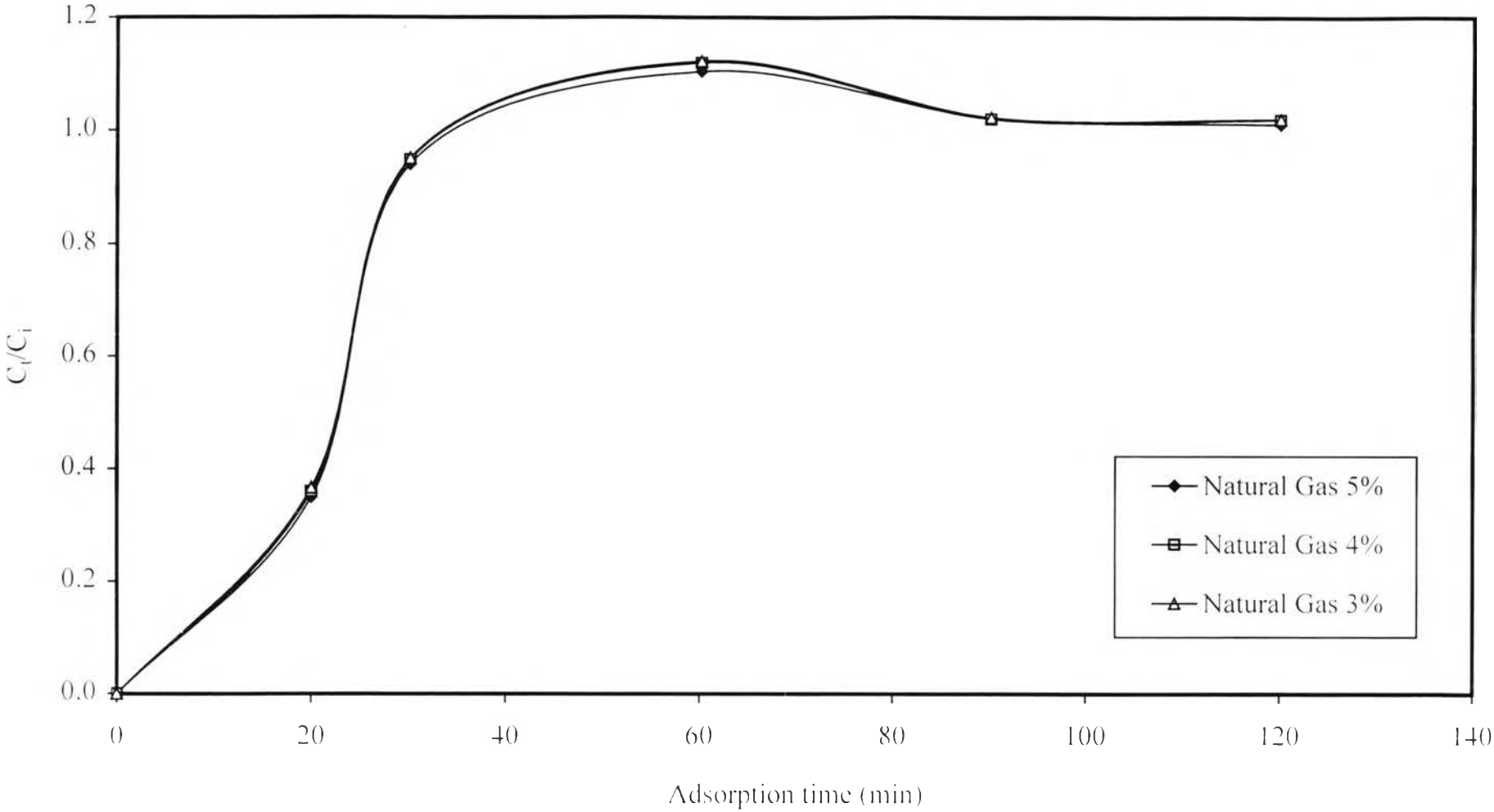

Figure 4.11 Breakthrough curves of pentane with different natural gas concentration.

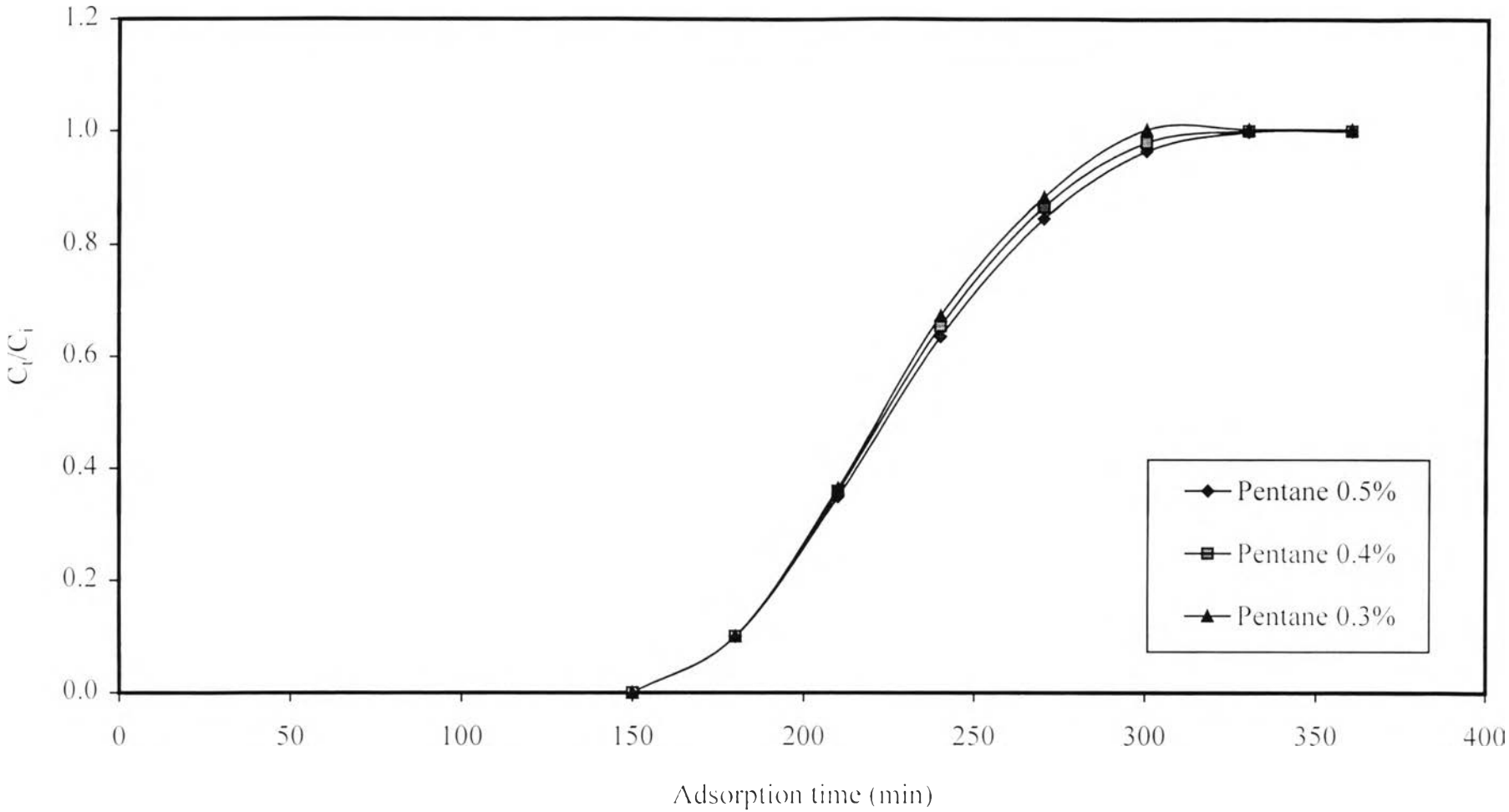

Figure 4.12 Breakthrough curves of water with different pentane concentration.

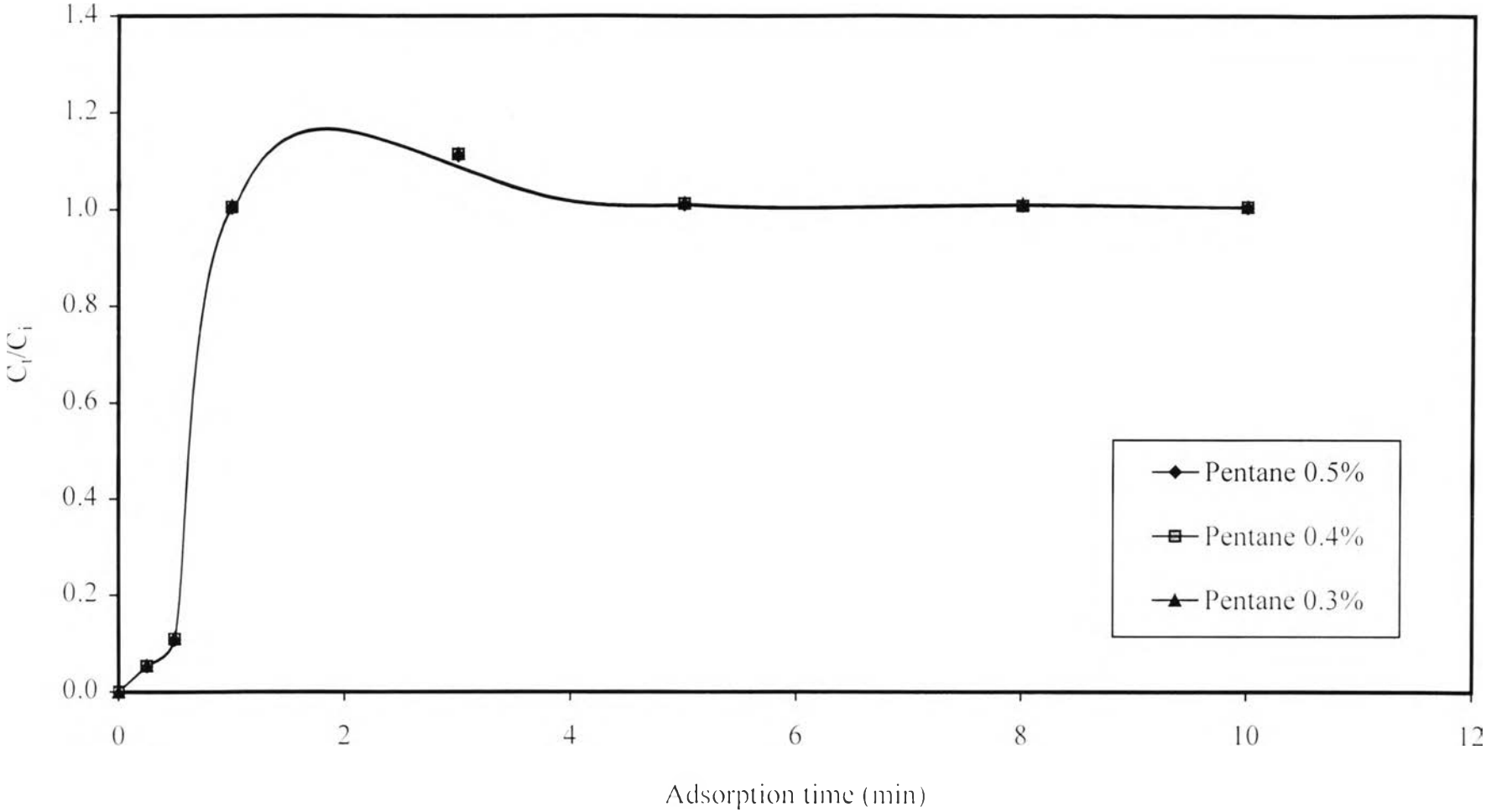

Figure 4.13 Breakthrough curves of methane with different pentane concentration.

physisorption and capillary condensation, which can be easily removed at the boiling point of each adsorbed component. Chemisorption, in fact, involves the formation of chemical bonding between the surface and the adsorbed species. So, the removal of chemisorped substances requires higher energy for breaking its chemical bonds than that of the physisorption needed.

After each adsorption process, the alumina was regenerated by heating the adsorbent bed to 250°C for two hours, under continuous nitrogen flow. Figure 4.15 shows the water adsorption capacity versus the numbers of experimental runs. The plot evidently indicated that there is little change in the water adsorption capacity. Up to 5% reduction of the water adsorption capacity was observed after ten times of adsorption cycle.

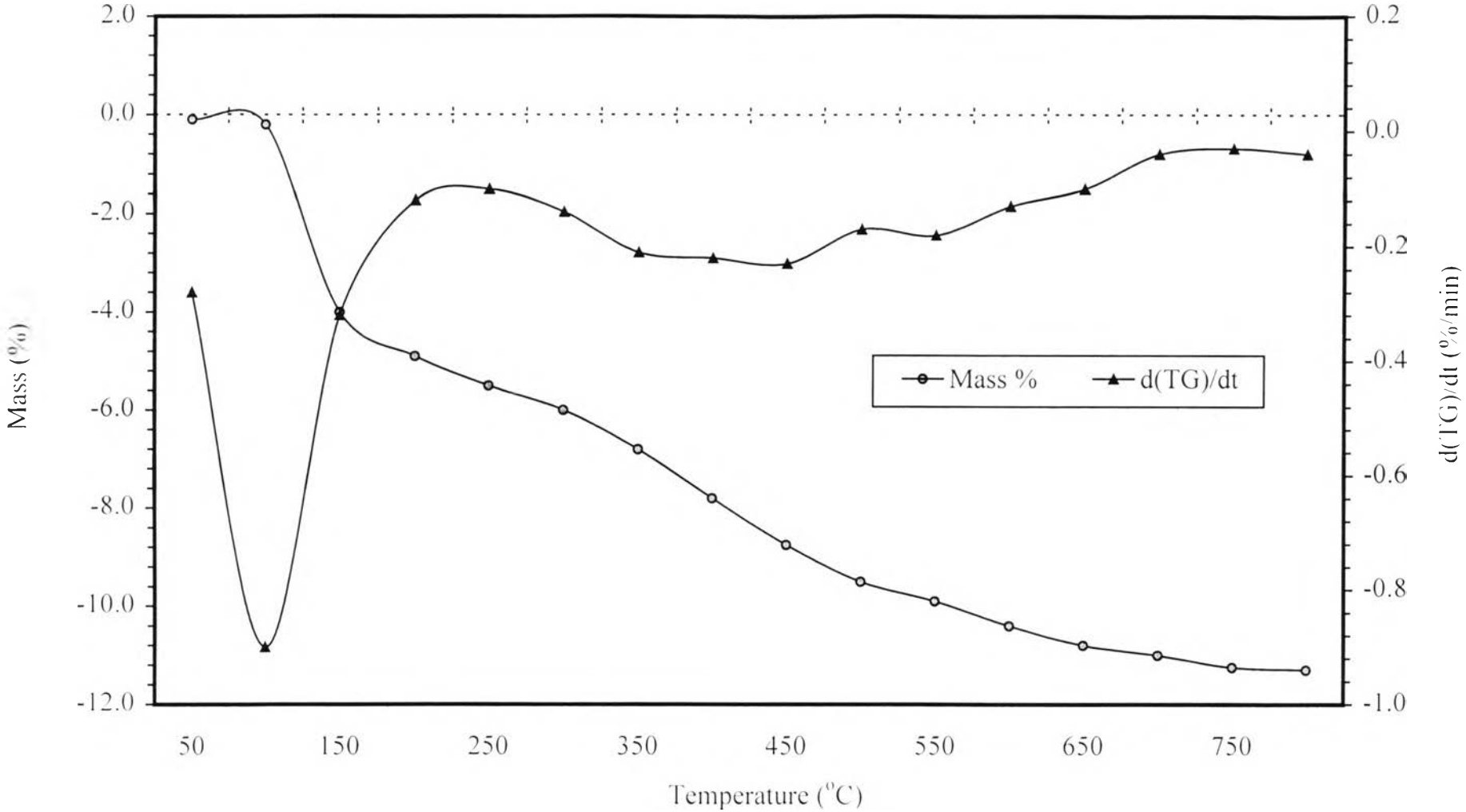

Figure 4.14 Thermogram of the water-saturated sol-gel alumina during the vacuum drying.

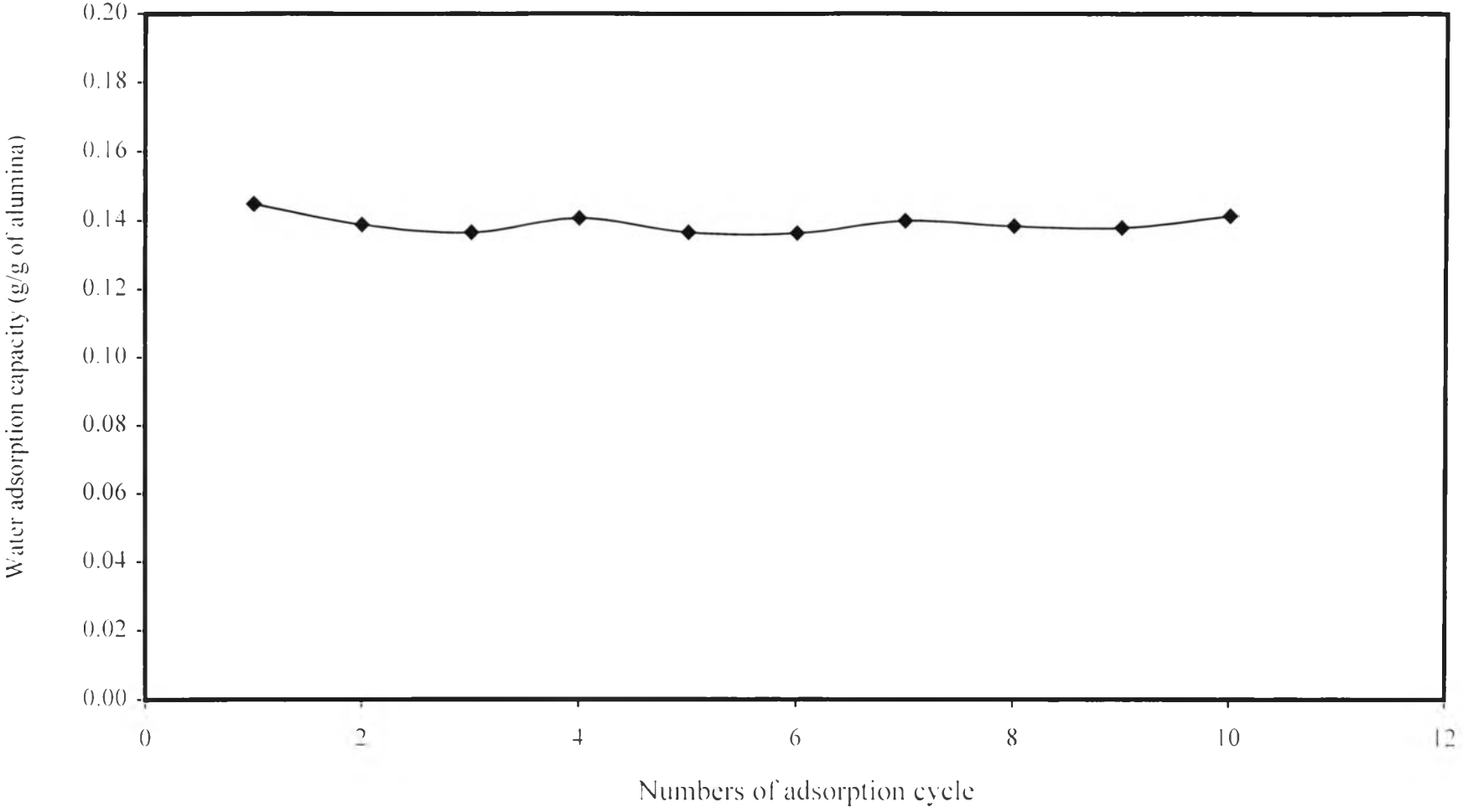

Figure 4.15 Water adsorption capacity of the sol-gel alumina during 10 adsorption cycles.